

MEASUREMENTS OF DISPERSION OF ULTRASONIC WAVE VELOCITY IN THIN LAYERS BY THE ULTRASONIC SPECTROSCOPY

W. WOJDOWSKI

Institute of Fundamental Technological Research
Polish Academy of Sciences
(00-049 Warszawa, Świątokrzyska 21)

This paper presents the results of measurements of the phase velocity dispersion of ultrasonic waves in thin aluminium sheets. The interaction between ultrasonic waves and a thin solid layer is analysed and the theoretical relations for the transmission and reflection coefficients are presented. Experiments are based on the spectrum analysis of ultrasonic pulses, generated by the broad-band probes in the frequency range of 2-13 MHz. From the maxima of transmission coefficients for different incidence angles the phase velocity of Lamb waves is determined as a function of ultrasonic wave frequency.

Presented method allows to determine the acoustic parameters and the dispersion curves for the velocity of Lamb waves in thin layers.

1. Introduction

The use of new materials in many branches of technology has been an incentive to further the ultrasonic methods of testing materials, especially those nonhomogeneous ones such as composites. Some of their properties, such as strength, resistance to fracture, thermal and electrical parameters largely depend on the current state of their internal structure. Suitable measurement techniques have therefore to be developed to assess the quality of such materials. It is the ultrasonic methods, based on the interaction of waves and nonhomogeneous media, that have found many applications in the field [1].

Complexity of phenomena that take place during the wave propagation in a multi-component medium is one of the reasons for the difficulties in proper interpretation of measurement results. The most difficult problem is to separate the geometrical effects that influence the ultrasonic wave parameters from those connected with the material structure and the boundary conditions at the interfaces of various materials. In particular, the response of laminates and adhesive connections is of interest since the relevant properties largely depend on the character of contacting surfaces. The measurement techniques are mainly based on the resonance in layers [2] and on the generation of

a number of Lamb wave modes [3, 4] caused by the incident ultrasonic wave. The Lamb waves are known to disperse considerably, i.e. their velocities are very sensitive to the frequencies. Dispersion curves are functions of material structure as well as boundary conditions on the surfaces. These, in turn, can vary with the changes in properties of glued connections and with the types of connected surfaces. Measurements of ultrasonic wave velocity dispersion are on the means to evaluate the quality of nonhomogeneous materials [4].

However, due to the complexity of involved phenomena and considerable difficulties in the interpretation of test data, some advanced measurement procedure must be employed in which the ultrasonic signals are analysed and digital data processing is used [5].

The present paper is devoted to the application of ultrasonic spectrum analysis in the determination of phase velocity dispersion curves for this layers of materials. The measurement apparatus and broad-band probes were used as described in [6, 7]. Measurement results are compared with theoretical predictions. Accuracy and resolution of the presented results are also assessed.

2. Transmission of ultrasonic waves through a thin material layer.

Basic theoretical relationships

The motion equation for the transmission of harmonic acoustic waves in an infinite isotropic medium has the form [8]

$$(\lambda + 2\mu)\Delta v + (\lambda + \mu)\nabla \times (\nabla \times v) = -\omega^2 \rho v \quad (1)$$

where λ , μ – Lamé's constants, v – particle velocity, ω – wave frequency, ρ – density of the medium. As known from the vector analysis, every vector field can be decomposed into two parts solenoidal and irrotational ones

$$v = v_1 + v_2 = \nabla \Phi + \nabla \times \Pi \quad (2)$$

where Φ and Π are the scalar and the vector potentials respectively. For the solenoidal field we have

$$\nabla \times v_1 = \nabla \times (\nabla \Phi) = 0 \quad (3)$$

whereas for the irrotational one the following applies:

$$\nabla v_2 = \nabla(\nabla \times \Pi) = 0 \quad (4)$$

The solenoidal field v_1 corresponds to a longitudinal acoustic wave, associated with volumetric changes of the medium, whereas the irrotational field v_L corresponds to a transverse, or shear, wave for which the volume remains constant. The equation (1) can be replaced by two equations for potentials Φ and Π

$$\begin{aligned} \Delta \Phi + k_L^2 \Phi &= 0 \\ \Delta \Pi + k_T^2 \Pi &= 0 \end{aligned} \quad (5)$$

where k_L – wave number for longitudinal wave, ($k_L = \omega/c_L$), k_T – wave number for shear

wave, ($k_T = \frac{\omega}{c_T}$, c_L and c_T – longitudinal and shear wave velocities in the medium, expressed in terms of Lamé's constants as

$$c_L = \sqrt{\frac{\lambda + 2\mu}{\rho}},$$

$$c_T = \sqrt{\frac{\mu}{\rho}}.$$

Consider a case in which an acoustic wave transmitted in a fluid medium impinges a solid isotropic layer of thickness h at an incidence angle θ . The direction of waves can be defined with the use of the wave vector \mathbf{k} , where $|\mathbf{k}| = \omega/c$ and c denotes the velocity of longitudinal waves in the fluid. To determine the transmission coefficient through the layer, the coordinate system and notation will be used as shown in Fig. 1. The longitudinal wave from the medium I impinges at an angle θ and is refracted in the layer (medium II) to be transmitted at an angle θ_L as a longitudinal wave and at an angle θ_T as a transverse wave. These waves are reflected at the lower and upper interfaces. A part of the wave energy is transmitted to the fluid medium III. Ratio of the amplitude in medium III to the amplitude of incident wave is a measure of the transmission coefficient through the layer.

Assume the media I and III to be identical and the longitudinal acoustic wave impinging in the x, z – plane (Fig. 1), i.e. the velocity components v_y vanish. According to the formula (2) the scalar potential Φ cannot depend on the coordinate y and the vector potential has to depend on Π_y only, $\Pi = [0, \Pi_y, 0]$.

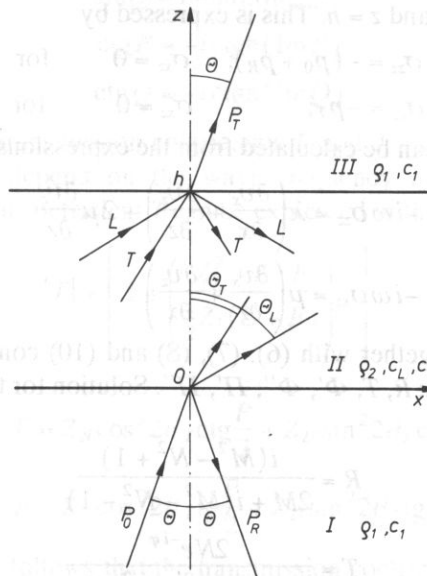


FIG. 1. Coordinate axes and notation for the transmission of ultrasonic waves through a layer.

Acoustic pressures of an incident, reflected and transmitted wave can be shown in the following forms:

$$\begin{aligned} p_0 &= \exp[ik_1(x \sin \theta + z \cos \theta)] \\ p_R &= R \exp[ik_1(x \sin \theta - z \cos \theta)] \\ p_T &= T \exp[ik_1(x \sin \theta + z \cos \theta)] \end{aligned} \quad (6)$$

where p_0, p_R, p_T are the pressure amplitudes of incident reflected and transmitted waves, respectively, R, T denote the reflection and transmission coefficients, $k_1 = \omega/c_1$ is a wave number for the medium I, c , is the wave velocity in the medium I.

The particle velocities in the layer can be derived from the formula (2) and calculated as

$$\begin{aligned} v_x &= \frac{\partial \Phi}{\partial x} - \frac{\partial \Pi_y}{\partial z} \\ v_z &= \frac{\partial \Phi}{\partial z} - \frac{\partial \Pi_y}{\partial x} \end{aligned} \quad (7)$$

The potentials Φ and Π for the transmission of waves in the layer have the form

$$\begin{aligned} \Phi &= \Phi' \exp[ik_L(x \sin \theta_L + z \cos \theta_L)] + \Phi'' \exp[ik_L(x \sin \theta_L - z \cos \theta_L)] \\ \Pi_y &= \Pi' \exp[ik_T(x \sin \theta_T + z \cos \theta_T)] + \Pi'' \exp[ik_T(x \sin \theta_T - z \cos \theta_T)] \end{aligned} \quad (8)$$

The angles $\theta, \theta_L, \theta_T$ satisfy the Snell's rule

$$k_L \sin \theta_L = k_T \sin \theta_T = k_1 \sin \theta.$$

The following boundary conditions must hold true at the interfaces between the media I, II and II, III: continuity of z -components of velocities and stresses and the absence of shearing stresses at $z = 0$ and $z = h$. This is expressed by

$$\begin{aligned} v_z^I &= v_z^{II}, & \sigma_{zz} &= -(p_0 + p_R); & \sigma_{xz} &= 0 & \text{for } z = 0, \\ v_z^{II} &= v_z^{III}; & \sigma_{zz} &= -p_T; & \sigma_{xz} &= 0 & \text{for } z = h. \end{aligned} \quad (9)$$

The stream components can be calculated from the expressions [8]

$$\begin{aligned} -i\omega \sigma_{zz} &= \lambda \left(\frac{\partial v_x}{\partial x} + \frac{\partial v_z}{\partial z} \right) + 2\mu \frac{\partial v_z}{\partial z} \\ -i\omega \sigma_{xz} &= \mu \left(\frac{\partial v_x}{\partial z} + \frac{\partial v_z}{\partial x} \right) \end{aligned} \quad (10)$$

The equations (9) together with (6), (7), (8) and (10) constitute a set of six linear equations in six unknown: $R, T, \Phi', \Phi'', \Pi', \Pi''$. Solution for the coefficients R and T is the following:

$$\begin{aligned} R &= \frac{i(M^2 - N^2 + 1)}{2M + i(M^2 - N^2 - 1)} \\ T &= \frac{2Ne^{-i\varphi}}{2M + i(M^2 - N^2 - 1)} \end{aligned} \quad (11)$$

where

$$\begin{aligned}
 N &= \frac{Z_{2l}}{Z_1} \frac{\cos^2 2\theta_T}{\sin P} + \frac{Z_{2T}}{Z_1} \frac{\sin^2 2\theta_T}{\sin Q} \\
 M &= \frac{Z_{2l}}{Z_1} \cos^2 2\theta_T \operatorname{ctg} P + \frac{Z_{2T}}{Z_1} \sin^2 2\theta_T \operatorname{ctg} Q \\
 \varphi &= k_1 h \cos \theta; \quad P = k_L h \cos \theta_L; \quad Q = k_T h \cos \theta_T \\
 Z_1 &= \frac{\rho_1 c_d}{\cos \theta}; \quad Z_{2l} = \frac{\rho_2 c_L}{\cos \theta_L}; \quad Z_{2T} = \frac{\rho_2 c_T}{\cos \theta_T} \\
 \cos \theta_L &= \sqrt{1 - \frac{c_L^2}{c_1^2} \sin^2 \theta}; \quad \cos \theta_T = \sqrt{1 - \frac{c_T^2}{c_1^2} \sin^2 \theta}
 \end{aligned}$$

When the incident angle θ is greater than the critical angle for either a longitudinal or transverse wave, the magnitudes $\cos \theta_L$ and $\cos \theta_T$ become purely imaginary and the following formulae should be used in the solution (11)

$$\begin{aligned}
 \cos \theta_L &= i \sqrt{\frac{c_L^2}{c_1^2} \sin^2 \theta - 1} \\
 \cos \theta_T &= i \sqrt{\frac{c_T^2}{c_1^2} \sin^2 \theta - 1} \\
 \sin P &= i \sinh(\operatorname{Im} P) \\
 \sin Q &= i \sinh(\operatorname{Im} Q) \\
 \operatorname{ctg} P &= -i \operatorname{ctgh}(\operatorname{Im} P) \\
 \operatorname{ctg} Q &= -i \operatorname{ctgh}(\operatorname{Im} Q)
 \end{aligned} \tag{12}$$

Both reflection and transmission coefficients R and T are complex numbers; their amplitudes and phases depend on the wave frequency $\omega = 2\pi f$. Using (11), the amplitude of transmission coefficient T can be expressed in the form [9]

$$|T| = \left[1 + \left(\frac{Z_1^2 - E \cdot F}{\frac{1}{2} Z_1 (E + F)} \right)^2 \right]^{-1} \tag{13}$$

where

$$\begin{aligned}
 E &= Z_{2l} \cos^2 2\theta_T \operatorname{ctg} \frac{P}{2} + Z_{2T} \sin^2 2\theta_T \operatorname{ctg} \frac{Q}{2} \\
 F &= Z_{2l} \cos^2 2\theta_T \operatorname{tg} \frac{P}{2} + Z_{2T} \sin^2 2\theta_T \operatorname{tg} \frac{Q}{2}
 \end{aligned} \tag{14}$$

From the formula (13) it follows that the transmission coefficient attains its maximum, i.e. equals unity, when

$$E \cdot F = Z_1^2 \quad (15)$$

In the case of acoustic impedance of a medium on both sides of the layer approaching zero ($Z_1 \approx 0$), the formula (15) furnishes $EF = 0$, that is either $E = 0$ or $F = 0$. Remembering (14), we arrive at the equations

$$\begin{aligned} \frac{\operatorname{ctg} \frac{P}{2}}{\operatorname{ctg} \frac{Q}{2}} &= -\frac{Z_{2T}}{Z_{2l}} \operatorname{tg}^2 2Q_T \\ \frac{\operatorname{tg} \frac{P}{2}}{\operatorname{tg} \frac{Q}{2}} &= -\frac{Z_{2T}}{Z_{2l}} \operatorname{tg}^2 2Q_T \end{aligned} \quad (16)$$

After a number of trigonometric rearrangements the equations (16) can be shown to be identical with the dispersion equations for the symmetric and antisymmetric modes of Lamb waves, presented in [10].

Thus, when the wave impedance of the solid layer is much larger than the impedance of the fluid from which the wave travels (i.e. Z , can be neglected in comparison with Z_{2L} and Z_{2T}) the maximum values of the transmission coefficient generate definite modes of Lamb waves in the layer. The above statement amounts to the so-called coincidence rule [9]. The amplitude of vibrations is at its largest for such incidence angles for which a resonance leads to the generation of a Lamb wave mode. The vibration energy is partially transmitted with relatively large amplitude are generated there. The transmission coefficient through the layer assumes its maximum value. The amplitude of reflected wave is also relatively large but, since its phase is opposite to that of the incident wave, the corresponding reflection coefficient attains its maximum.

When the maximum of the transmission coefficient corresponds to the incidence angle θ and the frequency f , a Lamb wave mode is generated in the layer. Projection of the incident wave vector is equal to the wave vector of the mode, Fig. 2. This means that

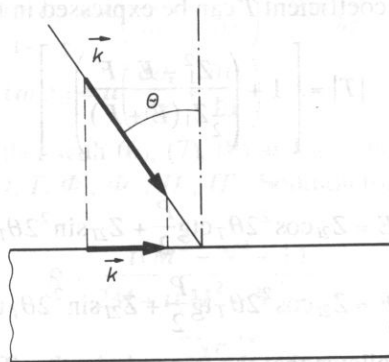


FIG. 2. Wave vector of Lamb wave k as a projection of incident wave vector k .

$|k_1| \sin \theta = |k|$, where $|k_1| = \frac{2\Pi f}{c_1}$; $|k| = \frac{2\Pi f}{c}$, c – phase velocity of the Lamb wave mode.

Hence

$$c = \frac{c_1}{\sin \theta} \quad (17)$$

Displacements of particles for a given mode of Lamb waves are given by the complicated expressions [10]. Qualitative and quantitative analyses of the motion of the medium transmitting Lamb waves are presented in [8]. Of special interest is the case in which the longitudinal wave impinges from the medium I at such an incidence angle that the resulting wave in the layer is transmitted at 45° , Fig. 3. In this case the mode is termed the Lamé mode [8] and consists of a purely transverse wave that is reflected at 45° from both faces of the layer. Simple geometrical relationships apply in this case:

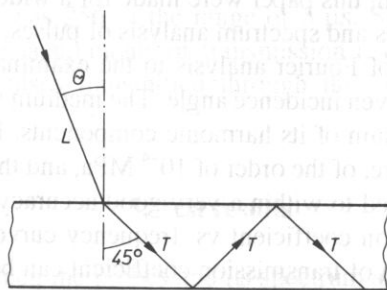


Fig. 3. Lamb mode - transverse wave travels in the layer at 45° .

$$\frac{\sin \theta}{c_1} = \frac{\sqrt{2}}{2c_T} \quad \text{– Snell's law}$$

$$\frac{2\Pi f}{c_T} \cdot \frac{\sqrt{2}}{2} = n \cdot \Pi, \quad n = 1, 2, 3 \quad \text{– boundary conditions on the layer interface [8].}$$

On combining the two above expressions, we get the formula

$$\sin \theta = \frac{n \cdot c_1}{2f \cdot h} \quad (18)$$

This is the condition for the incidence angle of longitudinal wave, expressed in terms of frequency, necessary for the transmission of a purely transverse wave inclined at 45° , i.e. the presence of Lamé's mode. This condition will be used further on to determine the velocities of transverse waves in solid layers.

3. Concept of measurements

The formula (17) determines the phase velocity of Lamb waves generated in a solid layer by a longitudinal ultrasonic wave impinging from a fluid at an angle θ . The wave velocity in the fluid is denoted by c_1 .

It follows from previous considerations that a given mode of Lamb waves can only be generated under specific frequency of incident waves and for a specific incidence angle. From the coincidence rule it follows that the maximum of transmission coefficient is associated with those magnitudes. Knowing the suitable incidence angle θ and the frequency f the phase velocity of Lamb mode can be calculated from (17). Lamb waves exhibit dispersion, i.e. their phase velocities depend on frequencies, see expressions (16).

Complete picture is complicated. Nevertheless, experimental determination of dispersion curves is possible with the help of various measuring techniques. In general, the reflection or the transmission coefficients are measured for fixed frequencies and various incidence angles [3, 9]. Relevant curves have a number of maxima or minima that correspond to successive Lamb modes. To obtain complete characteristics of velocity dispersions many ultrasonic probes must be available to emit waves with various frequencies.

Experiments described in this paper were made for a wide range of frequencies with the use of broad-band probes and spectrum analysis of pulses. The idea of measurements consists in the application of Fourier analysis to the examination of broad-band pulses generated in the layer at a given incidence angle. The medium is assumed to be linear, that is the ultrasonic pulse is a sum of its harmonic components. In the case of small amplitudes of the acoustic pressure, of the order of 10^{-4} MPa, and the wavelength of 1 mm, the linearity condition is satisfied to within a very good accuracy. The measurement results are presented as transmission coefficient vs. frequency curves. By broadly varying the incidence angle the maxima of transmission coefficient can be determined as depending on both the frequency and the incidence angle itself. Next, the formula (17) furnishes the phase velocity of Lamb waves for many modes simultaneously. As a result, the spectrum analysis method supplies a further picture of the velocity dispersion of Lamb waves than any other conventional method. It is also faster and more convenient to apply.

Computer program was prepared, based on the relationships shown in Sec. 2, to compare the test measurements of transmission coefficient with theoretical predictions. The following input data were used: impedance of the layer and the surrounding media, wave velocities in all the media concerned, thickness of the layer and the incidence angle. The transmission coefficient was computed from the formula (13). Three ranges of the incidence angle were distinguished: smaller than the first critical angle, in between the first and the second critical angle and larger than the second critical angle. In the last two cases the relationships (12) were used.

4. Measuring system

The test apparatus consisted of transmitting and receiving broad-band probes [7], ultrasonic defectoscope, sampling converter, micro-computer and printer [6]. The transmitting band was 2–13 MHz (with the drop of 12 dB). The setup is shown in Fig. 4. The incidence angle was changed with the use of micrometer screw to within an accuracy of 0.1° and in the range of 0 – 34° . The testpieces were made of aluminium sheet metal 0.5 and 1 mm thick, immersed in water.

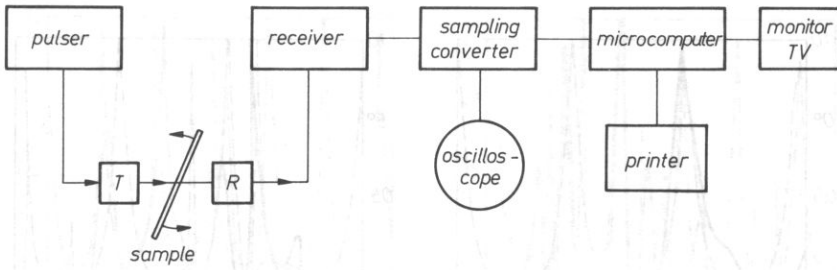


FIG. 4. Measuring set. T, R – broad-band transmitting and receiving probes.

Ultrasonic pulse transmitted through the layer was sampled and fed into the microcomputer. Fast procedure of Fourier transform enabled pulse spectra to be obtained. Sampling density was 256 in the range of $5 \mu\text{s}$. Spectral lines were spaced at 0.2 MHz; resolution of measurements of transmission coefficient maxima was about ± 0.1 MHz. Spectra of pulses transmitted through the layer were displayed on the monitor and printed.

5. Test results

Ultrasonic pulse between the probes and its spectrum are shown in Fig. 5. From the curves it follows that the useful range of frequencies is from 2 to 13 MHz. Its width is

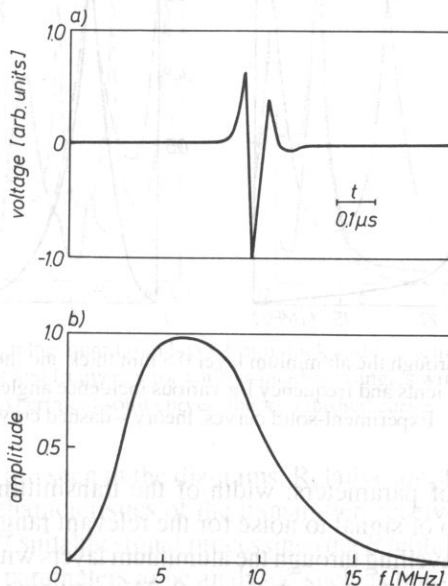


FIG. 5. a – Ultrasonic pulse between the probes at contact, b – its spectrum.

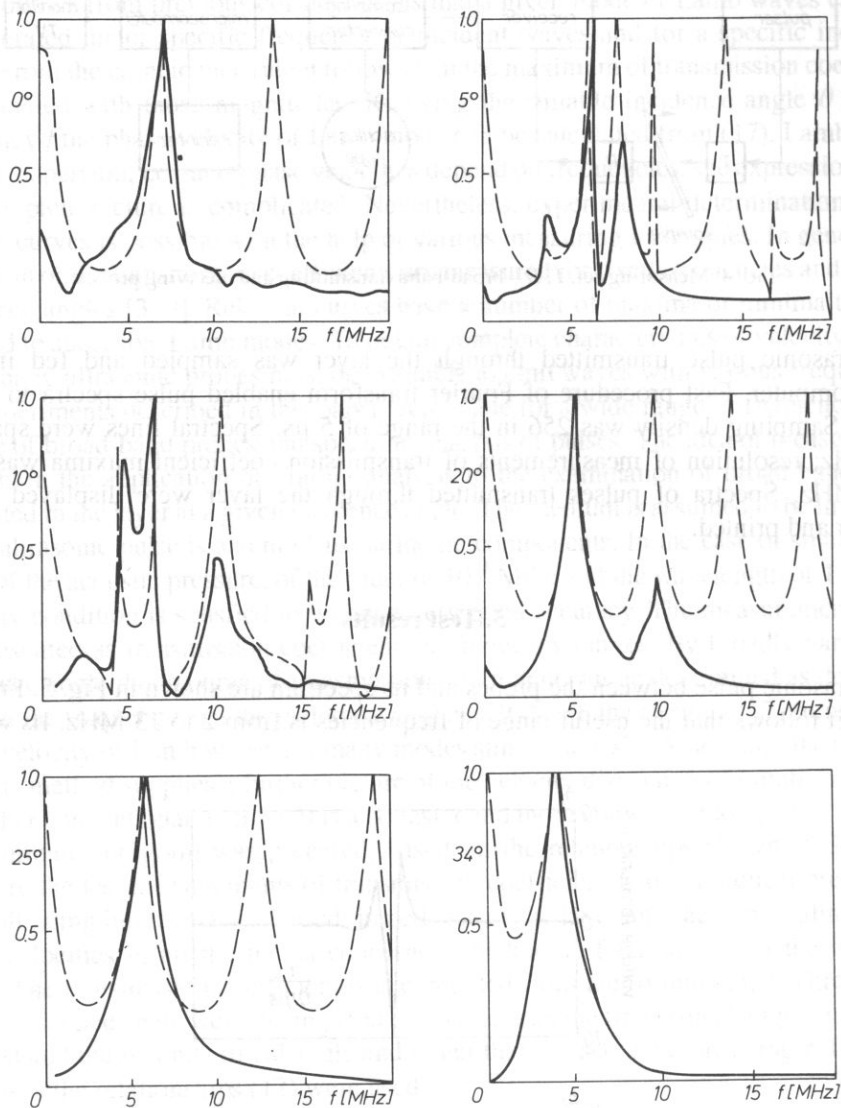


FIG. 6. Spectra of pulses through the aluminium layer 0.5 mm thick and theoretical relationships between the transmission coefficients and frequency for various incidence angles within the range of 0–34°. Experiment—solid curves, theory—dashed curves.

a result of a number of parameters: width of the transmitting band on pulser–probe–medium–receiver, ratio of signal to noise for the relevant range and sampling of signals.

Spectra of pulses travelling through the aluminium layers with thicknesses 0.5 and 1 mm at a number of incidence angles from the range 0–34° are shown in Figs. 6 and 7. Curves are also shown corresponding to the relationships between the transmission coefficients and frequencies, calculated with the use of computer program described in Sec. 4.

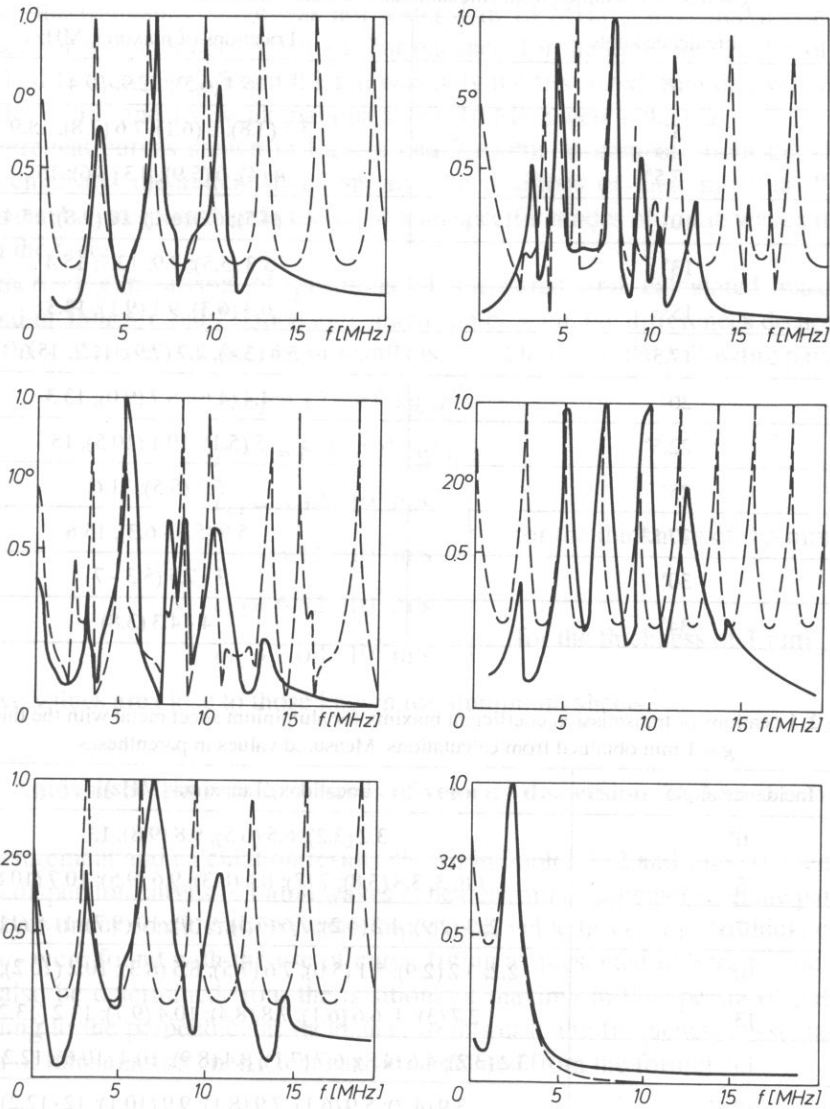


FIG. 7. Spectra of pulses through the aluminium layer 1 mm thick and theoretical relationships between the transmission coefficients and frequency for various incidence angles within the range of 0-34°.

Experiment solid curves, theory - dashed curves.

A number of maxima are seen in the diagrams. Relative amplitudes of those maxima depend on the spectrum characteristics of the transmitter-receiver system which can be accounted for by means of suitable signal processing (deconvolution process). However, this would require all the parameters to be analysed such as transmission band, damping in the medium and to on. Presentation of results is here confined to the transmitted pulses since their maxima were of primary interest.

Table 1. Locations of transmission coefficient maxima for aluminium sheet metal with the thickness $g = 0.5$ mm obtained from calculations. Measured values in parantheses

Incidence angle	Locations of maxima (MHz)
0°	6.4 (6.5); 12.9; 19.4
5°	3.7 (3.8); 6 (6.1); 7.6 (7.8); 13.9
7.5°	4 (4); 6 (5.9); 8.3 (8.6); 15
10°	4.4 (4.5); 6.3 (6.1); 10 (9.8); 15.4
13°	5.3 (5.5); 7.9; 13.7; 15.4
15°	6.3 (6.3); 9.1 (9.1); 13.3
17.5°	3.4 (3.8); 7.7 (7.9); 11.7; 15.6
20°	4.4 (4.6); 8.7 (9.0); 13.3
22.5°	5 (5.1); 10.1 (10.5); 15
25°	5.3 (5.5); 11.6
27.5°	5.9 (5.8 - 6.3); 15.8
30°	7 - 7.5 (5.3 - 7)
34°	4 - 4.3 (3.8)

Table 2. Locations of transmission coefficient maxima for aluminium sheet metal with the thickness $g = 1$ mm obtained from calculations. Measured values in parentheses

Incidence angle	Locations of maxima (MHz)
0°	3.2 (3.2); 6.5 (6.5); 9.8 (9.8); 13
5°	1.8; 3; 3.8 (3.8); 7 (7); 8.4 (8.3); 9.6 (9.5); 10.7 (10.8)
7.5°	2; 3 (2.9); 4.2 (4.2); 7.6 (7.5); 9 (9); 10 (9.7); 11.8 (11.7)
10°	2.2; 3.2 (2.9); 5.1 (5.0); 7.6 (7.5); 8.5 (8.3); 10.2 (10.2); 11.3
13°	2.7 (3); 4; 6.6 (6.1); 7.8 (8.4); 10.4 (9.7); 13.2 (13.2)
15°	3.2 (3.2); 4.6 (4.8); 6.7 (7.1); 8.4 (8.9); 10.4 (10.6); 12.2 (12.4)
17.5°	3.9 (4.2); 5.9 (6.1); 7.9 (8.1); 9.9 (10.1); 12 (12.2)
20°	2.2 (2.3); 4.4 (4.4); 6.7 (6.9); 8.9 (9.2); 11.2 (11.4)
22.5°	2.5 (2.6); 5.1 (5.4); 7.6 (7.9); 10.2 (10.5); 12.8 (13.2)
25°	2.7 (2.8); 5.9 (6.7); 9.1 (10.2)
27.5°	3 (3-3.4); 8
30°	3.7 (3.7)
34°	2 - 2.2 (2.1 - 2.3)

Since the frequency range was not wider than 13 MHz, higher maxima had small amplitudes or were not detected at all. For instance, for the incidence angles of 90° and 25° applied to the layer 0.5 mm thick it was only the first maximum that was obtained. For angles of 13° and 15° weak maxima above 10 MHz were detected.

Theoretical curves shown in Figs. 6 and 7 enable to compare both the shapes of experimental and theoretical diagrams and the positions of their maxima. Particular maxima can be interpreted and associated with specific modes of Lamb waves travelling through the layer.

Numerical comparison of positions of measured and calculated maxima are presented in Tables 1 and 2. Good agreement can be seen, the differences do not usually exceed 0.1–0.2 MHz. The best fit of results is found to be for the following parameters:

$$\rho_2 c_L = 17 \cdot 10^6 \text{ kg/m}^2\text{s}$$

$$\rho_2 c_T = 8.3 \cdot 10^6 \text{ kg/m}^2\text{s}$$

$$c_{L1} = 6.37 \cdot 10^3 \text{ m/s}$$

$$c_{T1} = 3.11 \cdot 10^3 \text{ m/s}$$

} for the thickness of 0.5 mm

$$c_{L2} = 6.32 \cdot 10^3 \text{ m/s}$$

$$c_{T2} = 3.08 \cdot 10^3 \text{ m/s}$$

} for the thickness of 1 mm

the above values are close to those known for aluminium sheets.

6. Analysis of test results. Curves of velocity dispersion for Lamb waves

Measurement and calculation results shown in Tables 1, 2 and Figs. 6, 7 enable the velocity dispersion curves of Lamb waves to be determined together with the parameters of the layer under consideration (wave impedance, velocities c_L , c_T and thickness. Both c_L and c_T were found with the use of curve-fitting as presented in Sec. 5. The velocity c_L can also be determined from the positions of maxima in the spectra of pulses corresponding to the perpendicular incidence. In this case the frequencies associated with maxima of transmission coefficient can be calculated from the formula

$$f_{\max} = \frac{n \cdot c_L}{2 \cdot h}, \quad n = 0, 1, 2, 3 \quad (19)$$

Given the thickness h , c_L readily follows from the above relationships. The transverse wave velocities can be determined due to the fact that, in the case of Lamb mode, a purely transverse wave propagates at 45° in the layer. Remembering (18) given in Sec. 2, the angle can be obtained as a function of the frequency at which the Lamb mode is generated. This condition, combined with the relationship between the location of transmission maximum and the frequency leads to the velocity c_T . This can be seen in Figs. 8 and 9 where the maxima from Figs. 6 and 7 are shown for various incidence angles and the condition (18) for Lamb modes is indicated. The incidence angles for which Lamb

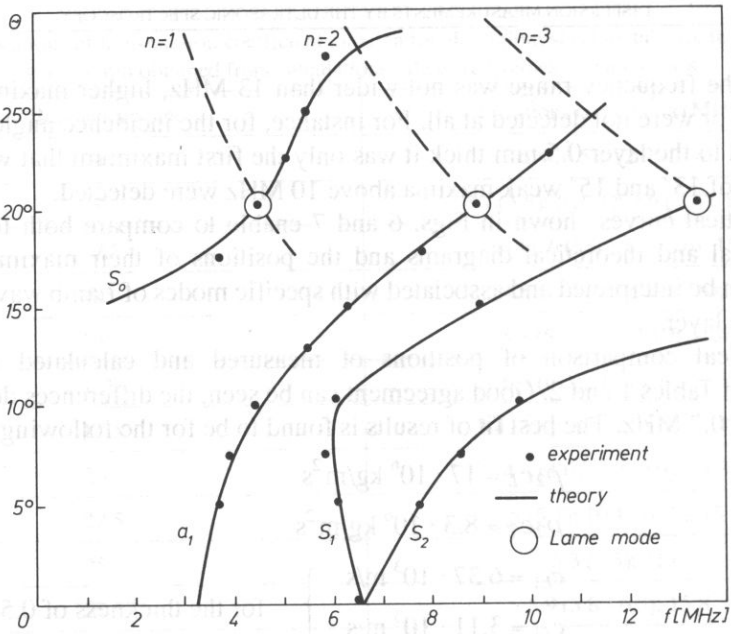


FIG. 8. Maxima of the transmission coefficient as a function of the incidence angle for the layer 0.5 mm thick. Curves applying to Lamb modes, formula (18) are shown dashed.

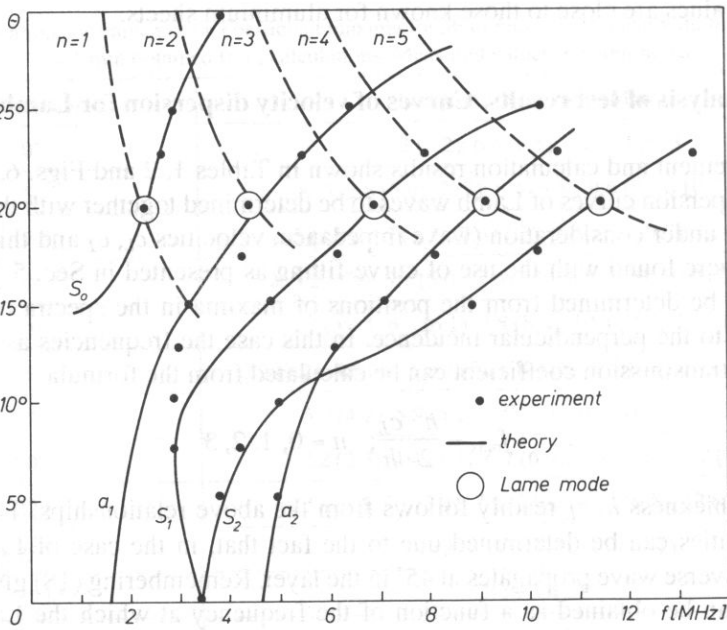


FIG. 9. Maxima of the transmission coefficient as a function of the incidence angle for the layer 1 mm thick. Curves applying to Lamb modes, formula (18), are shown dashed.

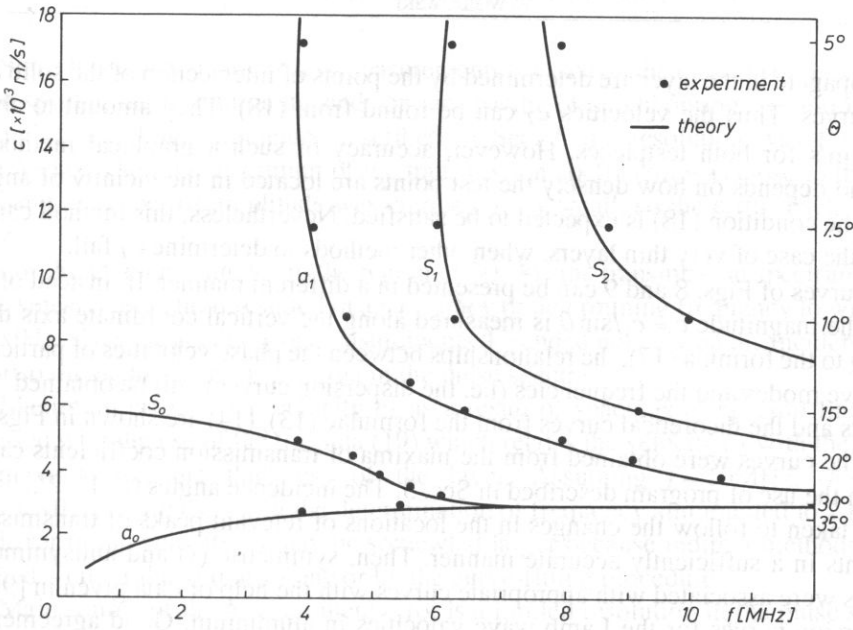


FIG. 10. Phase velocity dispersion curves for Lamb waves in the layer 0.5 mm thick.

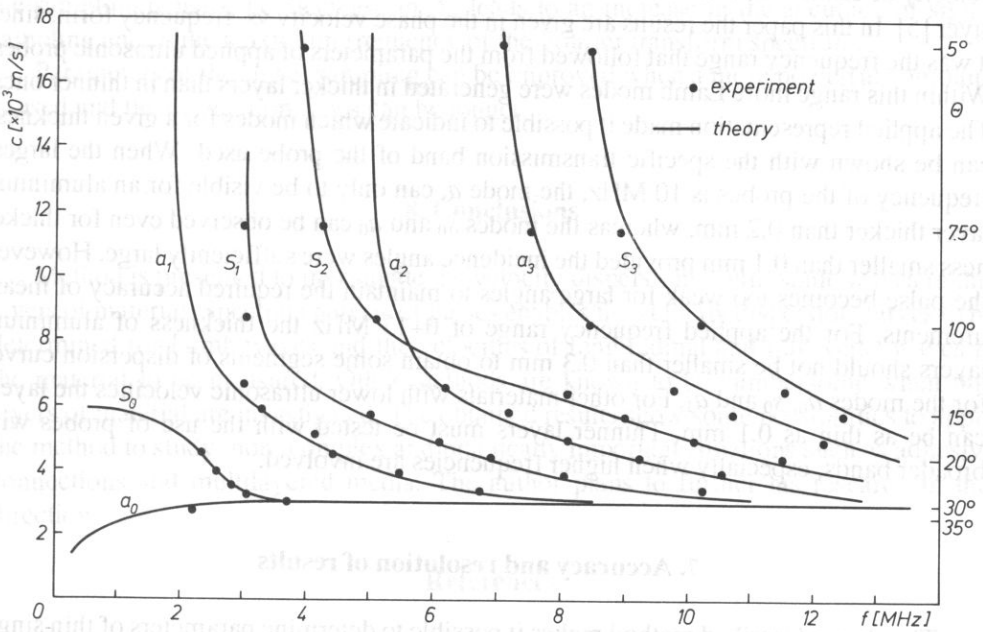


FIG. 11. Phase velocity dispersion curves for Lamb waves in the layer 1 mm thick

waves propagate in the layer are determined by the points of intersection of the solid and dashed curves. Thus the velocities c_T can be found from (18). They amount to about 3.1×10^3 m/s for both testpieces. However, accuracy of such a graphical method is limited and depends on how densely the test points are located in the vicinity of angles at which the condition (18) is expected to be satisfied. Nevertheless, this method can be useful in the case of very thin layers, when other methods to determine c_T fail.

The curves of Figs. 8 and 9 can be presented in a different manner. If, instead of the angle θ , the magnitude $c = c_1/\sin \theta$ is measured along the vertical coordinate axis then, according to the formula (17), the relationships between the phase velocities of particular Lamb wave modes and the frequencies (i.e. the dispersion curves) will be obtained. The test results and the theoretical curves from the formulae (13), (14) are shown in Figs. 10 and 11. The curves were obtained from the maxima of transmission coefficients calculated with the use of program described in Sec. 3. The incidence angles $0^\circ, 1^\circ, 2^\circ \dots$ up to 34° were taken to follow the changes in the locations of relevant peaks of transmission coefficients in a sufficiently accurate manner. Then, symmetric (s) and antisymmetric (a) modes were associated with appropriate curves with the help of data given in [9] for the dispersion curves for the Lamb wave velocities in aluminium. Good agreement is found between the measurements and the theoretical results. The differences do not exceed 0.1 ± 0.2 MHz, i.e., are within the accuracy of measurements.

It is common in the existing literature to represent the dispersion curves for the velocity of Lamb waves as a functions of a product of the frequency and the thickness of layer [5]. In this paper the results are given in the phase velocity vs. frequency form, since it was the frequency range that followed from the parameters of applied ultrasonic probes. Within this range more Lamb modes were generated in thicker layers than in thinner ones. The applied representation made it possible to indicate which modes for a given thickness can be shown with the specific transmission band of the probe used. When the largest frequency of the probes is 10 MHz, the mode a , can only to be visible for an aluminium layer thicker than 0.2 mm, whereas the modes s_0 and a_0 can be observed even for thickness smaller than 0.1 mm provided the incidence angles were sufficiently large. However, the pulse becomes too weak for large angles to maintain the required accuracy of measurements. For the applied frequency range of 0 ± 13 MHz the thickness of aluminium layers should not be smaller than 0.3 mm to obtain some segments of dispersion curves for the modes a_0, s_0 and a_1 . For other materials with lower ultrasonic velocities the layers can be as thin as 0.1 mm. Thinner layers must be tested with the use of probes with broader bands, especially when higher frequencies are involved.

7. Accuracy and resolution of results

The above described method makes it possible to determine parameters of thin single layers such as velocities of longitudinal and transverse acoustic waves. Phase velocity dispersion curves can also be found for various Lamb modes. It thus becomes necessary to evaluate the resolution and accuracy of the method.

Since the interpretation of test measurements is based on the location of maxima in the pulse spectra, the resolution depends on the spacing of neighbouring spectral lines. For the pulse sampling parameters described in Sec. 5 the resolution was found to be ± 0.1 MHz. When the maximum of the transmission coefficient was close to the ends of the band of probe, its amplitude was comparatively small, so the error reached 0.2–0.9 MHz.

For the incidence angles in the region of $30\div 34^\circ$ the transmission spectrum maxima were smeared out and it resulted in an accuracy of determining frequency to within 0.2–0.3 MHz. Thus the accuracy of measurements depended not only on the incidence angles but also on the locations of maxima in the pulse spectra.

Maximum error in the velocity c_L as a result of spacings of spectral lines can be assessed with the use of the formula (19) which relates the velocity c_L with the locations of maxima and the thickness of the layer. Assuming $f \approx 10$ MHz, $h \approx 0.5$ mm, $f \approx 0.1$ MHz, relative error in the determination of frequency amounted to 2 per cent.

Error in the velocity c_T may be somewhat larger because indirect methods are here applied – either the graphical one or by the curve-fitting procedure.

Main source of the measurement error is a limited resolution in the pulse sampling. Resolution and accuracy can be enhanced by increase in the length of the sampled signal and the density of sampling. Resolution of the frequency depends on the duration of sampled signal number of samples and is given by $\Delta f = 1/N \Delta t = 1/T$, where T is the signal period, N denotes the number of samples and Δt is their time spacing. Increase in the sampling density, i.e. decrease in Δt , leads to an increase in the accuracy of signal sampling and in the maximum frequency of the Fourier transform spectrum.

Parameters of the signal sampling can be improved when a more powerful computer is used and the calculation times can be longer.

8. Conclusions

Method is presented to investigate the velocity dispersion of ultrasonic waves in this layers of material. Spectral analysis of pulses enables the velocity dispersion curves to be determined for Lamb waves and the velocities of longitudinal and transverse waves in the material to be measured. Other methods are known to be cumbersome when thin layers of material are investigated. The obtained results show some possibilities to apply the method to study more complex and practically important situations such as adhesive connections and multilayered media. The author plans to further his research in this direction.

References

- [1] E.G. HENNEKE, J.C. DUKE JR., *Analytical ultrasonics for evaluation of composite material response*, Mat. Eval., **43**, 740–745 (1985).
- [2] I.C. COUCHMAN, F.H. CHANG, B.G. YEE, J.R. BELL, *Resonance splitting in ultrasonic spectroscopy*, IEEE Trans. Son. Ultr. **SU-25**, 293–300 (1978).

- [3] B. BRIDGE, R. SUDIN, *A study of high frequency Lamb wave propagation in very thin metal foils and plates*, British J. of NDT, **31**, 425–436 (1989).
- [4] A. PILARSKI, *Ultrasonic evaluation of the adhesion degree in layered joints*, Mat. Eval. **43**, 765–770 (1985).
- [5] W.R. SCOTT, P.F. GORDON, *Ultrasonic spectrum analysis for nondestructive testing of layered composite materials*, J. Acoust. Soc. Am., **62**, 108–116 (1977).
- [6] P. GUTKIEWICZ, Z. MOTYL, *Microcomputer system in frequency analysis of ultrasonic pulses* (in Polish) in Electric and Acoustic Methods of Investigations for Material and Biological Structures, IPPT-PAN, SEP, Warszawa–Jablonna, 305–319 (1984).
- [7] S. MACKIEWICZ, P. GUTKIEWICZ, Z. MOTYL, *Determination of damping coefficient for ultrasonic waves by spectral analysis of broad-band pulses* (in Polish), Materials of National Conf. of NDT, Szczecin 1987.
- [8] B.A. AULD, *Acoustic fields and waves in solids*, vol. 2, John Wiley and Sons, New York 1973.
- [9] L.M. BREKHOVSKIKH, *Waves in layered media*, Academic Press, New York 1960.
- [10] M. REDWOOD, *Mechanical waveguides*, Pergamon Press, Oxford 1960.

Received November 20, 1989; English version February 17, 1992